Available online at www.sciencedirect.com
SCIENCE DIRECT®
Journal of Chromatography A, 1042 (2004) 15–22
JOURNAL OF CHROMATOGRAPHY A
www.elsevier.com/locate/chroma

Direct zonal liquid chromatographic method for the kinetic study of actinomycin–DNA binding

Claire Vidal-Madjar [a,*], Florentina Cañada-Cañada [a,b], Ioanna Gherghi [c], Alain Jaulmes [a], Anastasia Pantazaki [d], Myriam Taverna [b]

[a] *Laboratoire de Recherche sur les Polymères, CNRS, 2 Rue Henry Dunant, 94320 Thiais, France*
[b] *Groupe de Chimie Analytique de Paris Sud, Faculté de Pharmacie, 92290 Châtenay-Malabry, France*
[c] *Laboratory of Analytical Chemistry, Aristotle University of Thessaloniki, 54006 Thessaloniki, Greece*
[d] *Laboratory of Biochemistry, Aristotle University of Thessaloniki, 54006 Thessaloniki, Greece*

Received 25 February 2004; received in revised form 12 May 2004; accepted 12 May 2004

Abstract

The binding of an anticancer drug (actinomycin D or ACTD) to double-stranded DNA (dsDNA) was studied by means of high-performance liquid chromatography (HPLC). ACTD is an antitumor antibiotic containing one chromophore group and two pentapeptidic lactone cycles that binds dsDNA. Incubations of ACTD with DNA were performed at physiological pH. The complexed and free ligand concentrations of the mixture were quantified at 440 nm from their separation on a size-exclusion chromatographic (SEC) column using the same buffer for the elution and the sample incubation. The DNA and the ACTD–DNA complexes were eluted at the column exclusion volume while the ligand was retained on the support. An apparent binding curve was obtained by plotting the amount emerging at the exclusion column volume against that eluted at free ACTD retention volume. A dissociating effect was evidenced and the binding parameters were significantly different from those obtained at equilibrium by visible absorbance titration. The equilibrium binding parameters determined by absorption spectroscopy were used as starting data in the numerical simulations of the chromatographic process. The results showed a strong dependency of the apparent binding parameters on the reaction kinetics. Finally the comparison of the apparent binding curve obtained from the HPLC experiments and from the numerical simulations permitted an evaluation of the dissociation rate constant ($k^d = 0.004\,s^{-1}$).

Keywords: Binding studies; Kinetic studies; Computer simulation; Actinomycins; DNA

1. Introduction

Actinomycin D (ACTD) is an important anticancer drug that binds to double-stranded DNA (dsDNA) via intercalation. The interaction between ACTD and DNA has been widely studied as the non-covalent ACTD–DNA complex is an interesting model for understanding the interactions between DNA and peptide-like substances [1]. It is now well recognized that its biological activity is related to its binding by intercalation to DNA.

The crystal structure of the DNA–ACTD complex has been studied by X-ray diffraction and a stereochemical model was proposed, in which the ACTD phenoxazone chromophore intercalates between the DNA base pairs [2,3]. It was shown that the pentapeptide lactone of the ACTD molecules interact with some specific DNA sequences. Systematic NMR spectroscopic studies [4,5] were used to investigate the interaction of ACTD with DNA sequences and were in good agreement with the above model. Spectral titration methods (visible absorbance, circular dichroism, fluorescence) have been also employed to study the binding of ACTD (or its fluorescent analogue) to DNA and to various DNA sequences [1,6–10]. Muller and Crothers [1] have shown that ACTD binds to dsDNA with high affinity and a very slow dissociation process of the DNA–ACTD complex was observed. The electrophoretic behavior of oligonucleotides in absence and in presence of ACTD have been studied by capillary electrophoresis (CE) [10] but the affinity constants were not determined by CE.

Several chromatographic methods were proposed to study the binding of a ligand to a macromolecule (for review,

* Corresponding author. Tel.: +33-1-49781219; fax: +33-1-49781323.
E-mail address: claire.vidal@glvt-cnrs.fr (C. Vidal-Madjar).

0021-9673/$ – see front matter © 2004 Elsevier B.V. All rights reserved.
doi:10.1016/j.chroma.2004.05.030

see [11,12]). In the direct zonal separation methods [13,14], the incubated species are separated and the free and bound ligand are quantified from the corresponding peaks. The method is valid only if there is no dissociation of the complex during its migration through the column [13–15]. Because of this limitation, the chromatographic method has been seldom employed to study ligand–substrate interactions [16–18]. Moreover in many of these experimental studies, the results may not have been adequately analyzed as the column dissociation effects were not accounted for.

The aim of this work was to investigate the potential of the direct separation method to characterize the binding affinity of ACTD to DNA. The direct separation methods are easier to carry out as a preincubated mixture containing the ligand and the macromolecule is injected into a size-exclusion chromatogaphic (SEC) column. As a continuous dissociation of the complex may occur during the elution in the column, an apparent binding curve is obtained, which describes the equilibrium between the interacting species only if the dissociation process is slow enough.

Numerical simulations of the chromatographic process were employed to test the validity of the method. In a previous work [15], we have developed a numerical algorithm with the hypothesis of an instantaneous equilibrium between the ligand and the biological macromolecule. In the present study, this model was modified to take into account the effects of association–dissociation kinetics. Computer simulation approaches including kinetic effects have already been described in literature [13,14] but were never applied to the interpretation of the apparent binding curves obtained when preincubated mixtures are analyzed by chromatography. The binding of DNA to ACTD represents an interesting experimental model to apply the direct separation HPLC method.

2. Theory

The association equilibrium between the ligand (L) and the DNA binding sites (S) can be described by a simple chemical equation:

$$L + S \underset{k^{\mathrm{d}}}{\overset{k^{\mathrm{a}}}{\rightleftarrows}} LS \tag{1}$$

The apparent adsorption and desorption rate constants are k^{a} and k^{d}, respectively. The dissociation equilibrium constant is $K_{\mathrm{D}} = k^{\mathrm{d}}/k^{\mathrm{a}}$. The concentration of bound ligand $[LS]$ is related to that of the free ligand $[L]$ by the equilibrium binding isotherm:

$$[LS] = Z[A]_0 \frac{[L]}{K_{\mathrm{D}} + [L]} \tag{2}$$

where $[A]_0$ is the total concentration of DNA in the solution and Z the stoichiometric coefficient of the reaction or number of binding sites per DNA molecule. It is related to the total concentration of binding sites in the solution ($c_0 = Z\,[A]_0$).

A numerical simulation method was used to generate the theoretical zone profiles corresponding to the elution of the total concentration of ligand from the column. The algorithm of the computer program includes two steps, one for the kinetic exchanges in solution and another for axial dispersion according to the Fick law. The size-exclusion column was divided into an arbitrary number of slices in which the above chemical equilibrium takes place. We assumed that the retentions of the species A and its complexes are governed by Henry law and are identical, while the ligand L was retained by the support. The hypothesis of a linear adsorption isotherm was also postulated for the interaction of the ligand with the adsorbent.

The phenomenon of size-exclusion is symbolized by the expression of the accessible volumes for the ligand (V_L^*) and for DNA and its complexes (V_A^*):

$$V_L^* = V_0 + \sigma_L V_{\mathrm{p}} = V_0(1 + k_L^0) \tag{3}$$

$$V_A^* = V_0 + \sigma_A V_{\mathrm{p}} = V_0(1 + k_A^0) \tag{4}$$

where V_0 is the excluded column volume and V_{p} the porous column volume. The permeation coefficients for species L and A are σ_L and σ_A, respectively. The corresponding permeation ratios are k_L^0 and k_A^0. In every slice, a strict mass conservation was kept. Thus the total concentrations of A (G_{A}) and L (G_{L}) remain constant and can be expressed as follows:

$$G_A = [A](1 + k_A)(1 + k_A^0) \tag{5}$$

$$G_L = [L](1 + k_L)(1 + k_L^0) + x(1 + k_A)(1 + k_A^0) \tag{6}$$

where $x = [LS]$ is the concentration of the bound ligand in the mobile phase. The solute capacity factors for species L and A are k_A and k_L, respectively.The process occurring in solution is then governed by the kinetic law:

$$\frac{\mathrm{d}x}{\mathrm{d}t} = r^{\mathrm{a}}(c_1 - x)(c_0 - x) - r^{\mathrm{d}}x \tag{7}$$

where the parameters are expressed as follows:

$$c_1 = \frac{G_L}{(1 + k_A)(1 + k_A^0)}, \quad r^a = \frac{k^a}{(1 + k_L)(1 + k_L^0)} \quad \text{and}$$

$$r^d = \frac{k^d}{(1 + k_A)(1 + k_A^0)}$$

The solution of Eq. (7) was applied to calculate the evolution of mobile and stationary phase compositions after a time Δt in each slice, the time needed by the mobile phase to flow through the volume of one slice.

The global dispersive effect was accounted for by applying the Fick law to the concentrations of each species in solution. It includes all the contributions to band broadening (molecular diffusion, eddy diffusion and kinetic mass transfers with the stationary phase). This global axial dispersion coefficient D is related [19,20] to the plate height (H) by $D = Hu/2$, where u is the velocity of the mobile phase. The

numerical procedures for simulating the Fick law were previously reported [15,21].

3. Experimental

3.1. Chemicals

ACTD (M_r = 1255.4, A-4262) and the highly polymerized dsDNA from calf thymus (D-1501) were purchased from Sigma (St. Louis, MO, USA). All other chemicals were from Aldrich (Milwaukee, WI, USA): tris(hydroxymethyl) aminomethane (25,285), sodium chloride (22,351-4). The buffers and solutions were prepared in Ultrapure water obtained from an Ultrapore Milli-Q water purification system (Millipore, Bedford, MA, USA).

3.2. DNA characterization

The dsDNA molecular mass was estimated by measuring its intrinsic viscosity from DNA solutions ranging from 0.1 to 1 g/L. The value found ($[\eta] = 145$ dL/g) permitted to estimate (the M_r of dsDNA (3.8×10^7)), when using the expression proposed by Crothers and Zimm [22] for high molecular mass DNA polymers. When calculating the mean number of base pairs (bp) per dsDNA molecule from its molecular mass, one finds 57,000 bp per DNA molecule.

3.3. Absorbance measurements at equilibrium

The binding measurements at equilibrium were performed using the method described in reference [1] with a Varian Cary 100 UV–vis spectrophotometer (Varian, Palo Alto, CA, USA). The concentration of the stock ACTD solutions were determined by measuring their absorbance in the buffer using an extinction coefficient of 24 500 M^{-1} cm^{-1} at 440 nm [6,7]. The extinction coefficient of bound ACTD at 440 nm (15 300 M^{-1} cm^{-1}) was determined from its spectrum measured in presence of a large DNA concentration (0.5 g/L) when the amount of free ACTD can be neglected. The maximum of this spectrum was shifted to 445 nm.

Various mixtures of known total concentrations of DNA (0.05 g/L) and ACTD (from 0.001 to 0.030 g/L) were prepared in 20 mM Tris–HCl buffer at pH 7.5. The mixtures were incubated and shaken for 2 h at ambient temperature. The absorbance changes at 440 nm were used to plot the bound versus free ACTD concentrations.

3.4. HPLC apparatus

The HPLC studies were performed with a system consisting of a LC-9A pump (Shimadzu, Kyoto, Japan), a Model 7125 sample injector (Rheodyne, Berkeley, CA, USA), fitted with a 100 μL sample loop. An optical scanning UV–vis detector (Spectra FOCUS, Spectra-Physics, San Jose, CA, USA) was routinely used. The detections of ACTD and of its associated forms with DNA were performed at 440 nm. When required, the monitoring wavelength of DNA peak was set at 260 nm. The signal from detector was connected to a data acquisition module (Hercule 2000, JMBS, Fontaine, France) and the chromatogram was stored via the Diamir software in the Personal Computer hard disk (Optilex GX1-MT, Dell, Austin, TX, USA). A Waters 996 photodiode-array detector (Waters, Milford, MA, USA) was used in preliminary experiments to obtain the spectrochromatogram of a DNA–ACTD sample mixture. The HPLC separations were performed with a TSK-gel G3000 SW (Tosohaas, Montgomeryville, PA, USA) SEC column (300 mm × 7.8 mm). The mobile phase (20 mM Tris–HCl buffer at pH 7.5) was delivered at a flow rate of 1 mL/min.

3.5. Chromatographic method

All reagents were diluted in the mobile phase buffer. The concentration of the ACTD stock solution was determined by measuring its absorbance at 440 nm, with the UV–vis spectrophotometer. Various ACTD–DNA solutions were prepared by mixing equal volumes of a DNA solution (0.1 g/L) with varying concentrations of ACTD solutions (from 0.01 to 0.025 g/L). The mixtures were incubated overnight by gentle shaking.

The study of the binding of ACTD to DNA was performed by injecting 100 μL of the incubated mixtures into the SEC column. A typical chromatogram recorded at 440 nm is shown in Fig. 1. The apparent binding curves were determined by plotting the amount of ACTD eluting in the first peak against that eluting in the second peak. The apparent concentrations in the incubated solution were calculated by dividing these amounts with the volume of sample injected. The chromatographic system was calibrated by injection of pure ACTD solutions at various concentrations and integra-

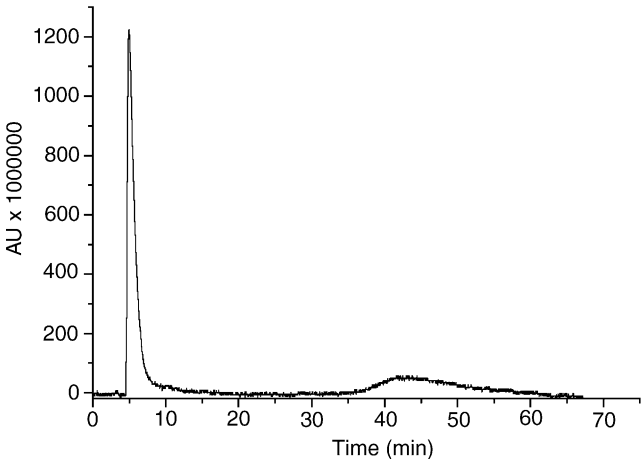

Fig. 1. Chromatogram of a preincubated ACTD–DNA mixture. Detection at 440 nm. Sample with $[DNA]_0 = 0.05$ g/L and $[ACTD]_0 = 0.015$ g/L TSK–gel G3000 SW (300 mm × 7.8 mm) SEC column. Flow rate: 1 ml/min. Buffer: 20 mM Tris–HCl buffer at pH 7.5.

tion of peak areas. The response of bound ACTD was calculated by dividing the response of free ACTD by the ratio (1.6) previously determined by spectrophotometry from the absorbance of bound ACTD in presence of a DNA excess.

3.6. Numerical procedures

The numerical simulation program was written in Fortran language and run on a Personal Computer. The method consists in subdividing the column into equally spaces cross-slices of arbitrary thickness. The chemical reactions and the exchanges between the phases of every slice were calculated with an increment of time equal to that needed for the eluent to flow through the slice. The number of slices selected were large enough to minimize numerical dispersion and thus to render its contribution negligible compared to the band broadening orginated from diffusion.

The experimental peak integrations were performed using the facilities of the Origin software (Microcal Software, Northampton, MA, USA). A non-linear least square fit program (Origin software) was used to determine the coefficients of the binding isotherms Eq. (2). The results are given together with the 95% confidence interval.

4. Results and discussion

4.1. Binding equilibrium isotherm from visible absorbance measurements

The binding equilibrium isotherm characterising the association of ACTD to dsDNA was determined by spectral titration at 440 nm. The coefficients of the binding equilibrium isotherm were determined from the best fit to equation 2 using a non-linear least square program. The values of $Z[A]_0$ and K_D are given in Table 1.

The asymptotic value $Z[A]_0 = 8.6\,\mu$mol/L yields 0.11 for the apparent number of binding sites per bp of DNA molecule. This data is in good agreement with that of reference [1] obtained by spectral analysis in neutral medium in presence of a buffer containing 0.18 mol/L NaCl. Muller and Crothers [1] observed an important decrease of the K_D equilibrium constant at increasing salt concentrations in the buffer. The K_D value determined in our work, is about half that obtained by Muller and Crothers [1]. The higher affinity observed in the present experiment is explained by the low ionic strength of the buffer employed.

Table 1
Equilibrium coefficients of the binding isotherm

Method	$Z[A]_0$[a] (μmol/L)	K_D (μmol/L)
UV–vis spectrophotometry (at equilibrium)	8.6 ± 0.3	0.20 ± 0.05
SEC separation[b] (apparent data)	2.4 ± 0.1	0.25 ± 0.05

Comparison of the results obtained by UV–vis spectrophotometry and HPLC analysis of the incubated sample.
[a] $[A]_0 = 0.05$ g/L $= 0.00132\,\mu$mol/L.
[b] Experimental conditions as described in Section 3.

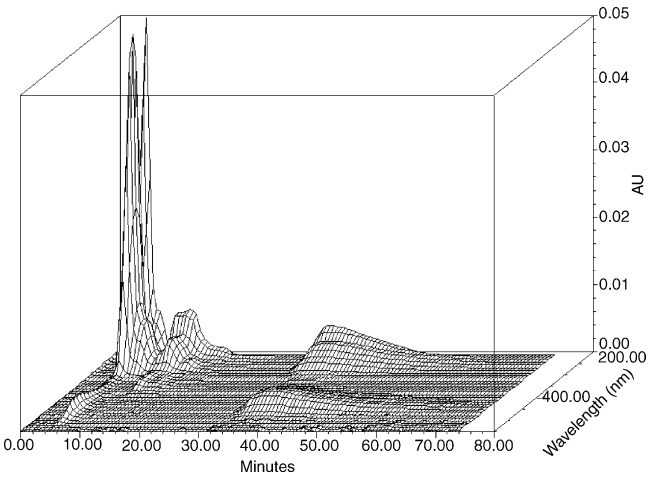

Fig. 2. Diode-array chromatogram of a preincubated ACTD–DNA mixture. Photodiode-array detection. Sample with $[DNA]_0 = 0.05$ g/L and $[ACTD]_0 = 0.05$ g/L. Other experimental conditions as in Fig. 1.

4.2. Apparent binding curve obtained by HPLC analysis

Preliminary studies were performed using a SEC column coupled to a diode array detector. The 3D view obtained from the injection of mixture of DNA (0.05 g/L) and ACTD (0.05 g/L) at equilibrium is shown in Fig. 2. At this large concentration excess of ACTD, a maximum concentration of bound ligand in the incubated mixture is reached, corresponding to the asymptotic region of the binding isotherm. There is a coelution of DNA and of the DNA–ACTD complex at the elution volume of the first peak. As expected, a coelution of both DNA and its associated form with ACTD at the column excluded volume (5 mL) was observed and the corresponding spectrum exhibits two maxima at 260 and 445 nm. Indeed the DNA mean M_r (3.8×10^7) is largely above the exclusion limit of the TSK3000 column used (70 000 for the M_r of dextrans). The second peak elutes with a large retention volume (around 40 mL) equal to the retention volume of free ACTD. Its spectrum presents a single maximum at 440 nm. The ACTD retention volume is much larger than expected for small molecules, as the total permeation volume of the SEC column was determined at 12 mL. The high retention observed for ACTD and the asymmetric peak shape were explained by strong adsorption interactions of ACTD with the stationary phase. The dissociation of the ACTD complexed form occurring during the chromatographic process could be monitored at 440 nm since the response in the visible region of the spectrum arised only from the phenoxazone chromophore of the drug (Fig. 1).

The amounts of bound and free ACTD eluted from the column were calculated from the areas of the first and second peaks using appropriate calibration factors for ACTD and

bound ACTD, respectively. Generally, these amounts are not those present in the sample injected as a dissociation of the complex may occur during the chromatographic process. The importance of this effect depends on the kinetic rates of the association–dissociation equilibrium. In the present case, the dissociation seems to be relatively slow as we observed no noticeable baseline drift between the first and the second peak. With a lower concentration of ACTD in the injected mixture, ($[DNA]_0 = 0.05$ g/L and $[ACTD]_0 < 0.01$ g/L) the amount of free ACTD cannot be detected as the signal of the second peak is hidden in the baseline noise.

An apparent binding curve was obtained by plotting the amounts of bound ACTD per unit sample loop volume against that of free ACTD apparently present at equilibrium in the mixture injected. Two apparent binding coefficients were determined (Table 1) from the non-linear least square fit of Eq. (2) to the experimental data. When comparing these coefficients with those determined by spectrophotometry at 440 nm, one can notice that the values of the equilibrium constants measured by both methods are in good agreement. A marked difference exists for the asymptotic values of the binding curve as $Z[A]_0$ is divided by more than 3, when determined by the HPLC method. Such a result indicates a slow dissociation of the associated complex during its elution through the column.

4.3. Simulation of the chromatographic process

The dissociation of the ligand–DNA complex can be predicted by numerical simulation of the chromatographic process accounting for the effects of association–dissociation kinetics. The numerical simulations were carried out with the values of the coefficients of the binding isotherm (Eq. 2) ($K_D = 0.2 \times 10^{-6}$ mol/L and $Z[A]_0 = 8.6 \times 10^{-6}$ mol/L) determined from equilibrium measurements obtained by spectral titration (Table 1). The sample mixture injected at the column inlet was assumed to be at equilibrium. The profile generated at the column outlet is that of the total ligand concentration, equal to the sum of free and bound ligand species. The parameters used in the simulation algorithm correspond to the experimental conditions of the HPLC separation with the SEC column ($V_0 = 5$ mL, $V_p = 7$ mL, $k_A = k_A^0 = 0$, $k_L = 2.33$, $k_L^0 = 1.4$, $D = 0.005\,cm^2/s$, flow rate: 1 mL/min). As DNA and its complexed form are not retained by the SEC column, small retention factors were used for both species.

Fig. 3 illustrates typical simulated chromatograms obtained when increasing ligand amounts are injected, keeping constant the total concentration of the macromolecular substance ($[A]_0 = 1.32 \times 10^{-9}$ mol/L). For this series of total ligand profiles emerging from the column, the desorption rate constant was set to $k^d = 0.005\,s^{-1}$. An apparent binding isotherm was obtained by plotting the area of the first peak per unit volume of sample injected versus that of the second peak. The area of these peaks corresponds to the amounts of bound and free ligand apparently present in the sample injected, respectively. When the desorption process is fast ($k^d > 0.05\,s^{-1}$), the first peak almost disappears and the total ligand concentration elutes as a single peak at free ligand elution time. Therefore, plotting an apparent binding isotherm is possible only when the desorption process is slow enough.

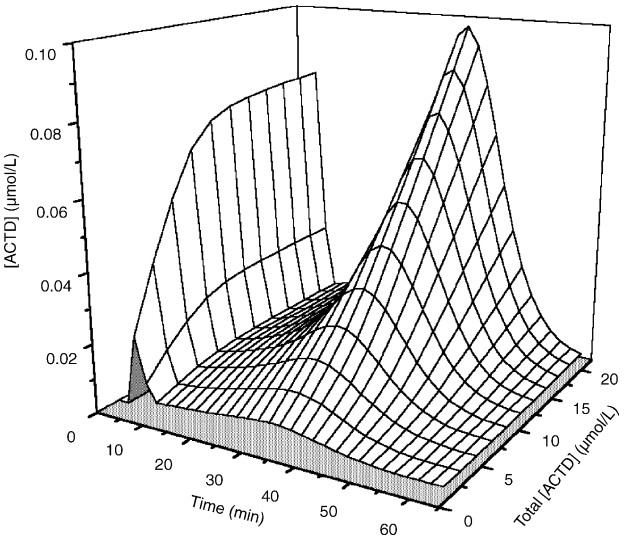

Fig. 3. Three-dimensional plot showing the evolution of the simulated total ligand profile as a function of the amount injected. Simulations performed with $2 < [L]_0 < 20$ µmol/L, $[A]_0 = 0.00132$ µmol/L, $Z = 6500$, $k^d = 0.005\,s^{-1}$ $V_0 = 5$ mL, $V_p = 7$ mL, $k_A = k_A^0 = 0$, $k_L = 2.33$, $k_L^0 = 1.4$, $D = 0.005\,cm^2/s$, flow rate 1 ml/min.

The influence of the desorption rate constant on the total ligand profile is shown in Fig. 4, when an excess of free ligand concentration is present in the sample injected. In the initial conditions of this simulation, the mixture contains a large total ligand concentration ($[L]_0 = 20 \times 10^{-6}$ mol/L) in equilibrium with the macromolecular substance ($[A]_0 = 1.32 \times 10^{-9}$ mol/L). With the selected binding isotherm ($K_D = 0.2$ µmol/L and $Z = 6500$), the concentrations of free and

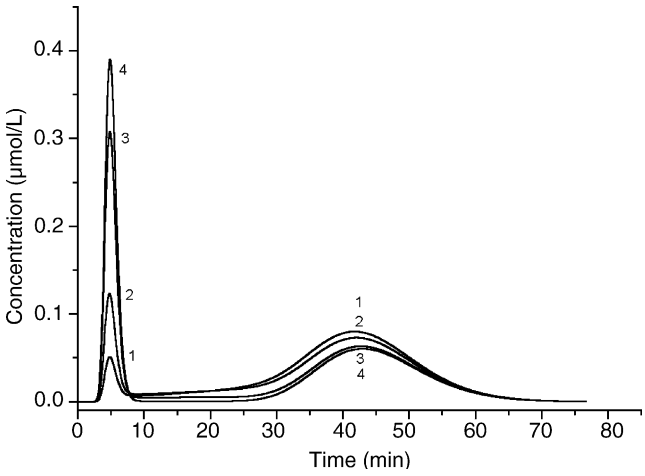

Fig. 4. Influence of the desorption rate constant on the simulated total ligand profile. Simulations performed with $[L]_0 = 20$ µmol/L, k^d (in s^{-1}) = 0.1 (1); 0.005 (2); 0.001 (3); 0.0001 (4) and the other parameters of Fig. 3.

bound ligand at equilibrium in the incubated sample are $[L] = 11.6 \times 10^{-6}$ mol/L and $[LD] = 8.4 \times 10^{-6}$ mol/L, respectively. In this case, the binding sites are almost totally saturated since this set of data corresponds to the asymptotic region of the binding isotherm.

With the above starting equilibrium and simulation conditions, we noticed a series of situations depending on the dissociation rate constants (Fig. 4). For extremely low values ($k^d < 10^{-4}\,s^{-1}$), the dissociating effect due to column dilution is negligible and the area of the bound ligand peak corresponds to the amount of complex in the sample. A decrease of this peak area is observed at larger k^d values, depicted by a signal slightly above the baseline between the first and second peak. For $k^d = 0.1\,s^{-1}$, the complex is almost totally dissociated and the first peak has nearly disappeared. This latter case is similar to the results simulated with the assumption of instantaneous equilibrium between bound and free species: a single symmetrical peak is obtained emerging at free ligand retention time.

In the range of relatively slow dissociating effects altering the amount of bound ligand eluted at the excluded column volume (from $k^d = 0.001$ to $0.01\,s^{-1}$) a retained peak emerges from the baseline, provided that the free ligand concentration in the injected sample is large enough. With the set of initial conditions of Fig. 3, the second peak is hidden in the baseline drift resulting from the dissociation of the complex when $[L]_0 < 8 \times 10^{-6}$ mol/L. The apparent binding curves of Fig. 5 were thus generated at sufficiently large total ligand concentration values ($[L]_0 > 8 \times 10^{-6}$ mol/L). The column dissociation effect was studied by changing the value of the desorption rate constant and the parameters of the apparent binding isotherm are listed in Table 2.

For an almost "irreversible" association process ($k^d < 0.0005\,s^{-1}$), the apparent binding curve nearly coincides with the theoretical equilibrium plot (Fig. 5). In this case, the parameters given in Table 2 are close to the equilibrium coefficients of Eq. (2). A decrease of the asymptotic value of the simulated apparent binding curve at increasing desorption rates is noticed in Fig. 5. On this figure is also reported the experimental binding curve determined by the

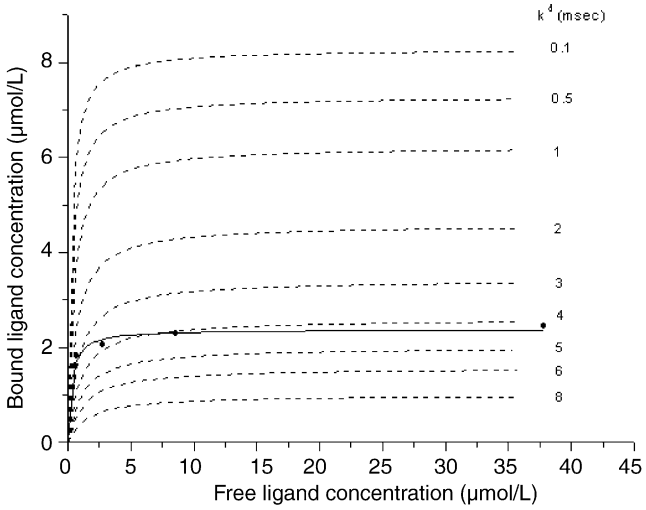

Fig. 5. Influence of the desorption rate constant on the apparent binding curve. Comparison with the experimental apparent ACTD–DNA binding curve: (•) and solid line: experiment (same conditions as in Fig. 1) and $0.0125 < [ACTD]_0 < 0.050$ g/L; (- - -) simulation with parameters of Fig. 3, $8 < [L]_0 < 40\,\mu$mol/L and $0.0001 < k^d < 0.01\,s^{-1}$.

direct separation method. The apparent stoichiometry of the ACTD–DNA association reaction measured with the HPLC method is quite low, much below the value expected from the equilibrium spectroscopic measurements. This discrepancy suggests a non-negligible dissociation process which is illustrated by the series of apparent theoretical binding curves of Fig. 5. The simulation which best describe the experimental apparent binding curve is that generated with a value of k^d around $0.004\,s^{-1}$. The association rate constant ($k^a \approx 2 \times 10^4\,L\,mol^{-1}\,s^{-1}$) was calculated from the ratio of k^d value and the equilibrium binding constant ($K_D = 0.2 \times 10^{-6}$ mol/L). This value of k^d is of the same order of magnitude order as that determined for the dissociation of the actinomycin C_3–DNA complex [1], using a detergent induced method. At high calf thymus DNA concentrations, Muller and Crothers [1] have found several discrete dissociation times, with the lowest at 570 s. A detergent-driven dissociation method was also used by Chen [6] to study the kinetics

Table 2
Simulation of the chromatographic process

k^d (s^{-1})	$Z[A]_0$ (µmol/L)	K_D (µmol/L)	$Z[A]_0$ (µmol/L)	K_D (µmol/L)
0.0001	8.29 ± 0.01	0.245 ± 0.005	8.46 ± 0.01	0.223 ± 0.005
0.0005	7.29 ± 0.03	0.32 ± 0.01	8.03 ± 0.01	0.230 ± 0.005
0.001	6.23 ± 0.03	0.42 ± 0.03	7.56 ± 0.01	0.25 ± 0.01
0.002	4.58 ± 0.03	0.60 ± 0.05	6.74 ± 0.02	0.28 ± 0.02
0.003	3.42 ± 0.03	0.8 ± 0.1	6.07 ± 0.03	0.31 ± 0.03
0.004	2.60 ± 0.02	0.9 ± 0.1	5.50 ± 0.03	0.33 ± 0.03
0.005	2.00 ± 0.02	1.1 ± 0.1	5.02 ± 0.03	0.35 ± 0.05
0.006	1.57 ± 0.01	1.2 ± 0.1	4.60 ± 0.05	0.40 ± 0.05
0.008	1.00 ± 0.01	1.5 ± 0.1	3.95 ± 0.05	0.43 ± 0.05
0.01	0.67 ± 0.01	1.8 ± 0.1	3.45 ± 0.05	0.45 ± 0.05
Simulation column volumes	$V_0 = 5$ mL and $V_p = 7$ mL		$V_0 = 1$ mL and $V_p = 1.4$ mL	

Influence of the desorption rate constant on the parameters of the apparent binding isotherm. Simulations with: $K_D = 0.20\,\mu$mol/L, $[A]_0 = 0.00132\,\mu$mol/L, $Z = 6500$, $k_A = k_A^0 = 0$, $k_L = 2.33$, $k_L^0 = 1.4$, $D = 0.005\,cm^2/s$, flow rate 1 ml/min.

of the interaction of ACTD with several self-complementary sequences. Larger dissociation times were found ranging from 3300 to 800 s.

The simulation of the chromatographic process has shown that the apparent binding parameters are greatly affected by the desorption process taking place when the associated form is migrating through the column. The analysis time was particularly long because a SEC column was used for separating the interacting species and an important column dissociation effect was noticed. It is interesting to test our approach for studying the ACTD–DNA binding system with shorter analysis times in order to reduce this effect. The simulation tests have shown (Table 2) that the discrepancies between apparent and theoretical binding curves are greatly reduced by increasing the speed of analysis with a column of smaller volume.

5. Conclusion

In this work, we have tested the potential of a direct separation chromatographic method for measuring the equilibrium binding constants of a ligand and a macromolecule substance present as a mixture in the injected sample. The apparent binding curve is close to the equilibrium binding-isotherm for interacting systems when extremely low dissociation rates occur. Because of non-negligible column dissociation effects, the direct separation method can only give a magnitude order of the association equilibrium constant. The apparent stoichiometric coefficient is also greatly affected by the dilution process occurring when the associated form is migrating through the column. Its value is largely underestimated at the experimental conditions used in this work for eluting the ACTD–DNA complex.

The approach remains interesting for the kinetic study of interacting systems which exhibit relatively slow desorption kinetics, as for ACTD and DNA. In this case, apparent experimental curves can be obtained from the amounts emerging at the retention times of the bound and free species. The desorption rate constant is then evaluated by fitting the simulated apparent experimental binding curves to the experimental ones. In the method proposed in this work, the equilibrium binding coefficients were determined from independent measurements as these parameters cannot be determined by the direct separation chromatographic method.

The simulations of the chromatographic process would be useful to define the conditions at which an association complex can be eluted from a column with a sufficiently low dissociation effect. Various experimental conditions could be defined to select the most appropriate ones for measuring the kinetic and equilibrium parameters from the apparent binding curve. Work is now in progress to improve the method. Indeed, increasing the speed of analysis would allow the method to be applied with accuracy to interacting systems that undergo slow dissociation during the separation analysis.

6. Nomenclature

c_0	total concentration of DNA binding sites (mol/L) $c_0 = Z[A]_0$
D	global dispersion coefficient (cm^2/s)
G_A	total concentration of DNA and its complexes in a column slice (mol/L)
G_L	total concentration of ligand in a column slice (mol/L)
H	theoretical plate height (cm)
k_A	capacity factor of DNA and its complexes
k_L	capacity factor of ligand
k^a	association rate constant ($L\,mol^{-1}\,s^{-1}$)
k^d	dissociation rate constant (s^{-1})
K_D	dissociation equilibrium constant (mol/L)
k_A^0	permeation ratio of DNA and its complexes
k_L^0	permeation ratio of ligand
r^a	global association rate constant ($L\,mol^{-1}\,s^{-1}$)
r^d	global dissociation rate constant (s^{-1})
[species]	concentration of the indicated species
$[species]_0$	total concentration of the indicated species
u	mobile phase velocity along column length (cm/s)
V_A^*	volume accessible to DNA and its complexes (mL)
V_L^*	volume accessible to the ligand molecules (mL)
V_P	pore volume in the column (mL)
V_0	excluded column volume (outside the pores) (mL)
Z	maximal number of ligand molecules bound to a DNA molecule
σ_A	permeation coefficient of DNA and its complexes
σ_L	permeation coefficient of the ligand molecules

Acknowledgements

The authors thank “La junta de Extremadura-Consejeria de Educacion, Ciencia y Tecnologia y el Fondo Social Europeo” for the postdoctoral fellowship given to F. Cañada-Cañada.

References

[1] W. Muller, D.M. Crothers, J. Mol. Biol. 35 (1968) 251.
[2] H.M. Sobell, S.C. Jain, T.D. Sakore, C.E. Nordman, Nature New Biol. 231 (1971) 200.
[3] H.M. Sobell, S.C. Jain, J. Mol. Biol. 68 (1972) 21.
[4] D.J. Patel, Biochemistry 13 (1974) 2396.
[5] H. Chen, X. Liu, D.J. Patel, J. Mol. Biol. 258 (1996) 457.
[6] F.M. Chen, Biochemistry 27 (1988) 1843.
[7] F.M. Chen, Biochemistry 31 (1992) 6223.
[8] R.M. Wadkins, T.M. Jovin, Biochemistry 30 (1991) 9469.
[9] R.M. Wadkins, B. Vladu, C.S. Tung, Biochemistry 37 (1998) 11915.

[10] F. Sha, F.M. Chen, Biophys. J. 79 (2000) 2095.
[11] B. Sebille, R. Zini, C. Vidal-Madjar, N. Thuaud, J.P. Tillement, J. Chromatogr. 531 (1990) 51.
[12] D.S. Hage, S.A. Tweed, J. Chromatogr. B 699 (1997) 499.
[13] A. Nimmo, A. Bauermeister, Biochem. J. 169 (1978) 437.
[14] F.J. Stevens, Biophys. J. 55 (1989) 1155.
[15] C. Vidal-Madjar, A. Jaulmes, B. Sebille, M.J. González, B. Jiménez, L.M. Hernández, J. Chromatogr. 584 (1992) 11.
[16] J.C.K. Loo, N. Jordan, A.H. Ngoc, J. Chromatogr. 305 (1984) 194.
[17] C.G. Sanny, J.A. Price, Anal. Biochem. 246 (1997) 7.
[18] L.C. Santora, Z. Kaymakcalan, P. Sakorafas, I.S. Krull, K. Grant, Anal. Biochem. 299 (2001) 119.
[19] J.C. Giddings, Dynamics of Chromatography, Marcel Dekker, New York, 1965.
[20] F.H. Arnold, H.W Blanch, C.R. Wilke, Chem. Eng. J. 30 (1985) B25.
[21] A. Jaulmes, C. Vidal-Madjar, Anal. Chem. 63 (1991) 1165.
[22] D.M. Crothers, B.H. Zimm, J. Mol. Biol. 12 (1965) 525.